［投稿: 研究ノート］

Establishment of a Method for Inducing Pulmonary Fibrosis in *Xenopus laevis* Using an Ultrasonic Nebulizer

超音波ネブライザーを用いたアフリカツメガエルにおける肺線維症誘発手法の確立

Takanari Kida
Fourth year, Faculty of Policy Management, Keio University
木田 隆成
慶應義塾大学総合政策学部 4 年

Takumi Morikawa
Former Master's Program in the Graduate School of Media and Governance, Keio University
森川 拓海
元・慶應義塾大学大学院政策・メディア研究科修士課程

Masamichi Yamada
CSO, Human Life CORD JAPAN Inc.
山田 眞路
ヒューマンライフコード株式会社・研究開発担当

Masamitsu Harata
President and CEO, Human Life CORD JAPAN Inc.
原田 雅充
ヒューマンライフコード株式会社・代表取締役社長

Hiroki Kuroda
Professor, Faculty of Environment and Information Studies, Keio University
黒田 裕樹
慶應義塾大学環境情報学部教授
Correspondence to: hkuroda@keio.jp

Abstract:
***Xenopus* laevis, also known as the African clawed frog (hereafter referred to as *Xenopus*), is a widely used model organism and is considered a promising alternative to mammalian disease models. In this study, we modified the nebulizer component of a commercially available ultrasonic humidifier to develop a system for administering specific gases to *Xenopus*. Using this system, we administered bleomycin, a known inducer of pulmonary fibrosis, and observed its effects on the lungs. Four days after inhalation, significant lung shrinkage and inflammation were observed. This system has the potential to serve as a novel pathological model using adult amphibians in future research.**

代表的な実験モデル生物であるアフリカツメガエル(以下、ツメガエル)は、哺乳類の病気モデルの代替として有望視されている。本研究では、市販の超音波式加湿器のネブライザー部品を改良し、ツメガエルに任意の気体を吸入させるシステムを構築した。このシステムを用いて、肺線維症を誘発する薬剤であるブレオマイシンを吸入させ、肺への影響を観察した。その結果、吸入開始から 4 日後に、顕著な肺の縮小および炎症が確認された。今後、このシステムは、両生類成体を用いた新しい病理モデルとしての応用が期待される。

Keywords:
African clawed frog, *Xenopus laevis*, disease model, bleomycin, pathological model
アフリカツメガエル、ブレオマイシン、病理モデル

1. Introduction

Experimental model organisms are specific species widely used in biological research to understand basic biological processes (particularly those related to genes, cells, and physiological processes) and to discover universal principles that can be applied to other organisms.

Xenopus is known as one of the most excellent experimental model organisms. Particularly in the field of medical research, the use of *Xenopus* has shown remarkable progress in recent years, with its versatility in embryonic manipulation, as well as applications in genome editing techniques like CRISPR/Cas9 and some reporter assays (Nenni et al., 2019). Although *Xenopus* breathes through its lungs as an adult, the relationship between the respiratory system structures in *Xenopus* and the human esophagus, trachea, and bronchi is comparable. It has been reported that the lungs of *Xenopus* are comparable at the cellular and signaling levels to those of the mouse embryo at 8.5-10.5 days (Rankin et al., 2015). In the visceral system of mice, the heart has two atria and two ventricles, and the lung structure is also asymmetrical, so the distribution of lung lesions tends to be asymmetrical (Warburton et al., 2010). On the other hand, in the visceral system of *Xenopus*, the heart has two atria and one ventricle, and there is no need to consider left ventricular hypertrophy. Moreover, as the distance from the heart to the lungs is farther compared to mammals, it is thought that the lung structure remains symmetrical. Even if an effect appears in only one lung, it is necessary to consider that most mammals are originally

asymmetrical, but in the case of *Xenopus*, it is considered symmetrical, so there is no need to account for that factor.

The antitumor antibiotic bleomycin (BLM), synthesized by the bacterium *Streptomyces verticillus*, damages cells by inducing single-strand or double-strand DNA breaks, leading to cell cycle arrest and direct cellular damage (Stubbe and Kozarich, 1987). As a result, necrosis and apoptosis occur in epithelial and endothelial cells, triggering pulmonary inflammation, which can ultimately lead to the development of pulmonary fibrosis (Umezawa, 1974). In the mouse lung, there is a pathological model where BLM administration induces damage to alveolar cells and acute inflammation, leading to pulmonary fibrosis (Moeller et al., 2007; Dietert et al., 2017). However, in recent years, regulations on the use of mammals as experimental animals have been tightening, and the establishment of systems using experimental animals from non-mammalian vertebrate classes is being sought (Alves-Pimenta et al., 2024). We considered that establishing a model that induces pulmonary fibrosis using bleomycin in *Xenopus* would further expand the utility of *Xenopus* as an excellent experimental animal.

Therefore, in this study, we first designed a new experimental system to administer aerosol to *Xenopus* and then aimed to establish a pathological disease model of pulmonary fibrosis in *Xenopus* through BLM administration.

2. Methods

2.1 Target for air mist administration

To administer air mist efficiently, it is necessary to select an appropriate size. The smaller the size, the less air mist is required, but if the size is too small, technical difficulties may arise. After conducting several preliminary experiments, it was determined that individuals with a body length of approximately 40 mm, measured from the tip of the head to the base of the hindlimbs, are appropriate (Fig. 1A). This corresponds to the minimum size that allows for blood sampling from the blood vessels. The internal abdominal structure of *Xenopus* of this size is shown in Fig. 1B. It can be seen that the lung structures are located on both sides of the body. In this study, when removing the lungs, we used a method in which the lungs were excised together with the esophageal section (Fig. 1C), and then only the lungs were isolated from that section.

2.2 Air mist inhalation method for *Xenopus*

In mouse experiments, tubular instruments called sondes and nebulizers are used for drug administration into the lungs (Shen et al., 2021; Sanjeewa et al., 2019). We decided to create a simple homemade nebulizer for drug administration to *Xenopus*. The procedure for creating it is as follows: We removed the vibrating component from a commercially available ultrasonic humidifier (Plastic bottle humidifier, #4550480003665, DAISO) and suspended it on a stand (Fig. 2A, B). The ultrasonic vibrating part was positioned facing downward to release aerosolized reagents (Fig. 2C). *Xenopus* was held by hand to

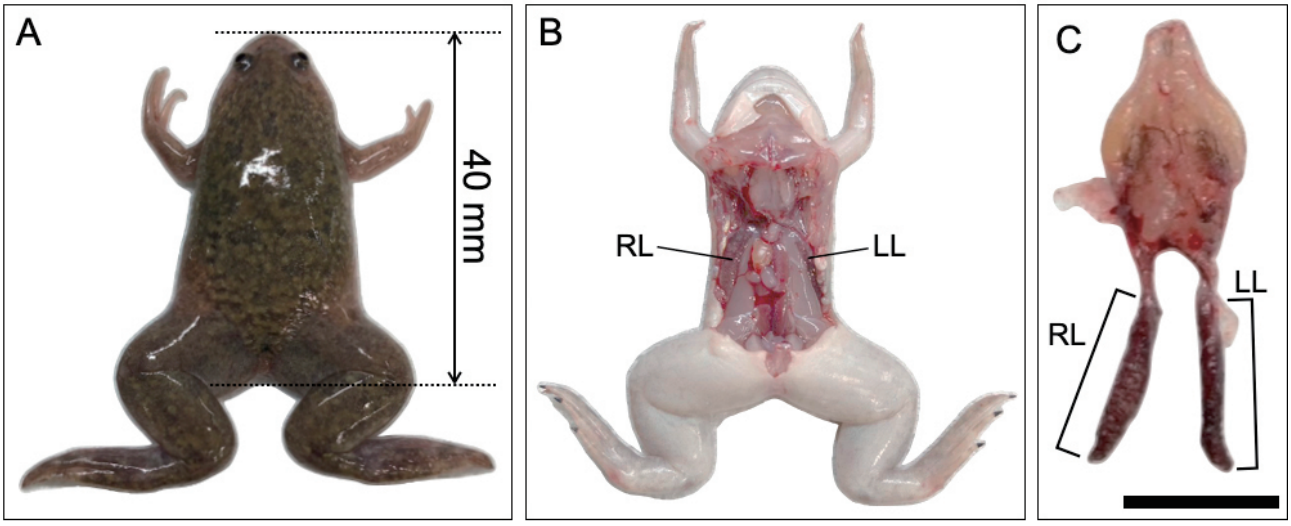

Fig. 1 *Xenopus* used in the experiment in this study and lungs connected to the esophagus and bronchi
(A) *Xenopus* used for drug administration through the oral cavity. Individuals with a body length of approximately 40 mm, measured from the tip of the head to the base of the hindlimbs, were used. (B) The internal structure of the abdomen in *Xenopus* of this size. Upon dissection of the abdomen, it can be seen that lungs of equal size are symmetrically present on both sides. RL, right lung; LL, left lung. (C) Lungs connected to the esophagus. To avoid damaging the lung tissue, the lungs were removed together with the esophagus, and then the lung portion was isolated. Scale bar: 1cm.

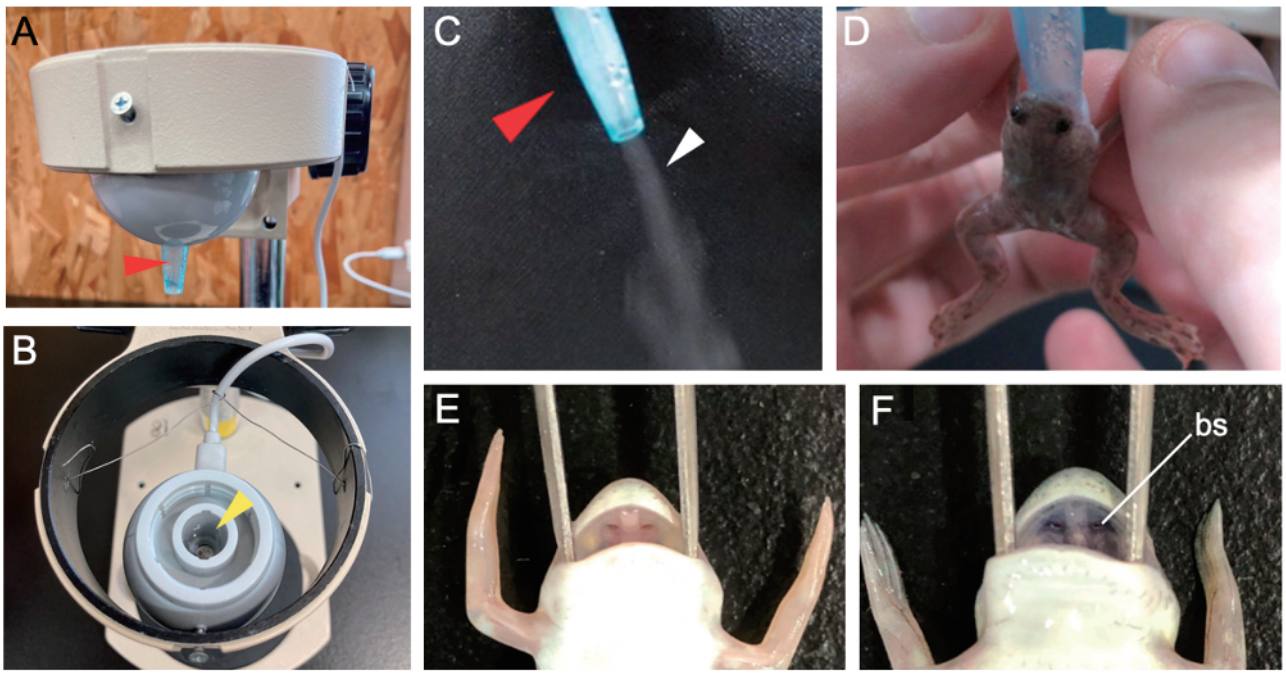

Fig. 2 Method for administering aerosol to *Xenopus* using a homemade nebulizer
(A) Ultrasonic vibrating component removed from a commercially available ultrasonic humidifier and attached to the frame of a stereomicroscope. A 100-1000 µL micropipette tip (P1000), with the front 2 cm section cut off, was used to insert into the oral cavity (red arrowhead). (B) Top view of A. Reagents can be placed in the central depression (yellow arrowhead). (C) Aerosolized liquid. White aerosol (white arrowhead) is seen being released from the tip of the micropipette for administration (red arrowhead). (D) *Xenopus* grasping the administration pipette. When the micropipette tip is pressed against the frog's mouth, it reflexively bites the micropipette tip. (E) Control for F. Oral cavity after administering aerosolized distilled water. (F) Oral cavity after administering aerosolized distilled water containing methylene blue. Blue-stained areas (bs, blue stained) can be observed inside the oral cavity.

open its mouth, and the tip of the tube was inserted into the mouth to allow it to inhale the aerosol (Fig. 2D). For comparison, we set up a control group in which 80 µL of water was administered to *Xenopus*, and a test group in which 80 µL of 0.1 mg/mL of BLM (bleomycin sulfate, #B3972, Tokyo Chemical Industry) was administered. The dosage was calculated based on the body weight ratio of mice, and considering the residual reagent inside the simple nebulizer, an additional 20 µL of water was administered to both the control and BLM groups after inhalation. Drug residue in the oral cavity was confirmed using aerosol containing methylene blue, a blue dye. When aerosol containing methylene blue was inhaled, the oral cavity turned blue (Fig. 2E, F). Drug administration was carried out inside a draft chamber.

2.3 Histological experiment

Xenopus was anesthetized by cooling on ice, and the lungs were removed using dissection scissors and forceps. To avoid damaging the left and right lungs, the lungs were excised from the base of the trachea, including the esophagus, and trimmed. The lungs were placed in a φ90 mm petri dish containing physiological saline. A vial was prepared, filled with a formalin solution made by mixing phosphate-buffered saline (PBS) and formaldehyde (FA) in a 9:1 ratio. The lungs were placed in the vial, rotated for 2 hours to fix them, and transferred to a vial filled with 70 % ethanol, where they were rotated again for 1 hour. Subsequently, they were transferred to 100 % methanol and rotated for 1 hour. The lungs were moved to a petri dish containing 100 % methanol, left to stand for 10 minutes, and placed in 100 % ethanol for 10 minutes, xylene for 30 minutes, and paraffin for 15 minutes to dehydrate and embed the tissues in paraffin. After embedding, the tissues were sliced to a thickness of 10 µm using a microtome. The sections were placed on a glass slide on a paraffin stretcher set at 50 ℃ and stretched on approximately 2 mL of distilled water at around 50 ℃ for about 15 minutes. Afterward, the water was removed using a Kimwipe, and the slides were left to air dry at about 50 ℃ for about 1 hour. The paraffin stretcher was turned off, and the slides were allowed to dry completely at room temperature overnight. Next, the paraffin sections attached to the slide glass were placed in a staining rack. Using a Coplin jar, the sections were immersed for 10 minutes in xylene, 2 minutes in 100 % ethanol, 1 minute in 70 % ethanol, 5 minutes in tap water, 30 seconds in hematoxylin, 15 minutes in running water, 15 minutes in 50-60 ℃ tap water, 1 minute in eosin, 5 seconds in 70 % ethanol, 5 seconds in 100 % ethanol, 2 minutes in 100 % ethanol, and

finally 4 minutes in xylene. The staining method using hematoxylin and eosin (HE) will hereafter be referred to as HE staining. Lastly, a cover glass was placed over the sections using Canada balsam (mounting medium), and after the mounting medium had dried, the samples were observed.

3. Results

3.1 Lung shrinkage caused by BLM administration

The lungs of *Xenopus* are symmetrical, with no differences in size or other characteristics. In this study, since no differences were observed between the left and right lungs, data were collected focusing only on the left lung. BLM is known as a drug that effectively induces pulmonary fibrosis in mammals and other organisms. If BLM affects the lungs of *Xenopus*, remarkable effects on the lungs are expected. In this study, lungs were removed from *Xenopus* one day, four days, and two weeks after BLM administration for observation. As a result, a noticeable difference was observed in the lungs of *Xenopus* treated with distilled water or BLM four days after administration. For convenience, the former will be referred to as "Control lung" and the latter as "BLM-treated lung."

In the Control lung, the lung showed no difference in shape or size compared to the lungs of normal individuals (Fig. 3A). On the other hand, in the BLM-treated lung, the lung was clearly smaller and had a reddish color (Fig. 3B). This suggests that congestion had occurred in the lung. The distance between the two ends of the lung was measured using an ocular micrometer to quantify the differences. The results showed that the average distance in the Control lung was 9.83 mm, whereas in the BLM-treated lung, it was 6.78 mm (Fig. 3C). This indicates that the BLM-treated lung was reduced by about 30 % compared to the Control lung. Interestingly, this difference had diminished after two weeks (data not shown). Additionally, none of the individuals died even after being kept for about two months. While urodeles such as newts exhibit strong regenerative abilities in their internal organs (Odelberg, 2005), *Xenopus* may also possess similar capabilities.

3.2 BLM administration leads to thickening of alveolar walls and decrease in their number

In addition to pulmonary fibrosis, symptoms of pulmonary fibrosis include thickening of the alveolar interstitium, hypertrophy of alveolar walls, and a reduction in the number of alveoli (Wolters et al., 2014). Therefore, to verify whether these symptoms can be observed following BLM administration to *Xenopus*, tissue sections were prepared, and the internal structure was examined. For the Control lung, a tissue section cut at the site indicated by the dotted line in Fig. 3A is shown in

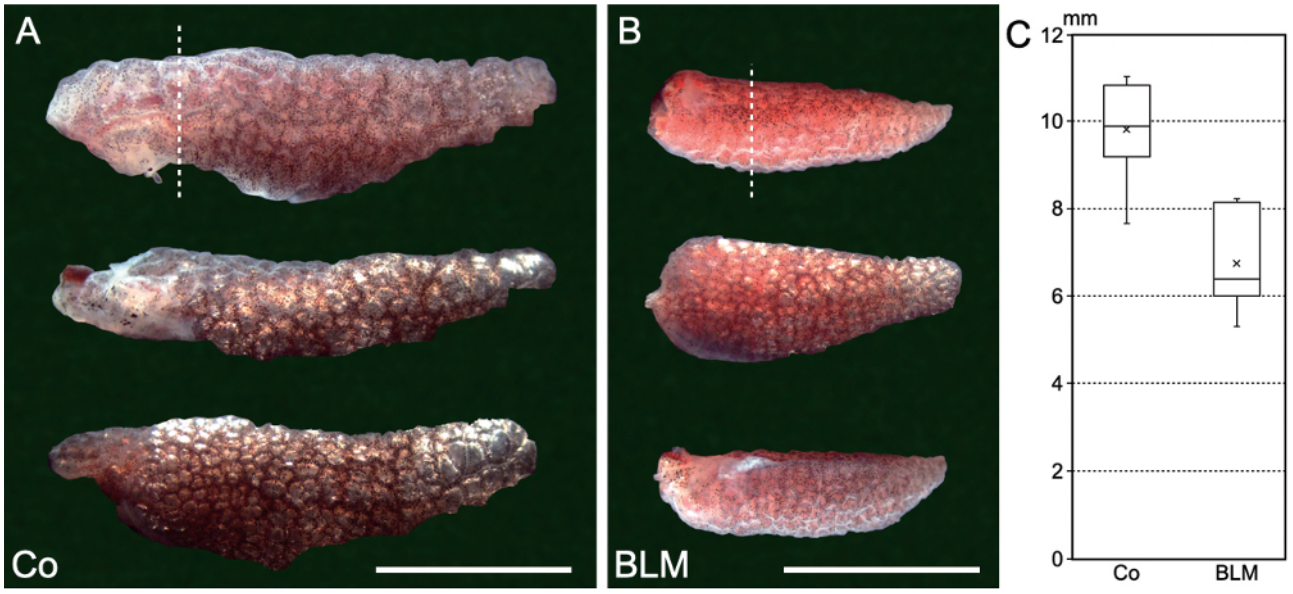

Fig. 3 Lung shrinkage in the BLM-treated group

(A) Control for B (Co). Left lungs excised from *Xenopus* four days after distilled water administration. Three typical-sized lungs are shown in parallel. Scale bar: 5 mm. The tissue sections cut along the dotted line are shown in Fig. 4. (B) Left lungs excised from *Xenopus* four days after BLM administration. Three typical-sized lungs are shown in parallel. Significant shrinkage compared to the Control is clearly observed. Scale bar: 5 mm. Additionally, compared to the Control, the lungs were congested and all exhibited a reddish hue. The tissue sections cut along the dotted line are shown in Fig. 4. In both cases, no difference was observed between the right and left lungs, so only the left lung results are presented. (C) Lung size comparison. The sizes of six left lungs were compared. The average size was 9.83 mm for the Control lung, while it was 6.78 mm for the BLM-treated lung (both n=6, $p < 0.001$). Thus, the size of the BLM-treated lung was reduced by approximately 30 % compared to the Control lung.

Fig. 4A. The internal structure was similar to that of a normal lung, with alveoli, pulmonary vessels such as pulmonary artery and veins, and stroma clearly visible (Fig. 4A shows each of these parts). For the BLM-treated lung, a tissue section cut at the site indicated by the dotted line in Fig. 3B is shown in Fig. 4B. In the BLM-treated lung, alveoli, pulmonary vessels, and stroma, as seen in the Control lung, were also identified. However, there was a noticeable reduction in the number of alveoli, and hypertrophy of the alveolar walls was observed on the surface of the alveoli. Additionally, the tissue section appeared overall redder. Since congestion was observed in the external appearance (Fig. 3), this may be related. Using image analysis software ImageJ, the cross-sectional area of the thickest regions in each tissue section was compared (Fig. 4C). The average value for the Control lung (n=15) was 7.21 mm^2, while the value for the BLM-treated lung (n=15) was 4.63 mm^2. In other words, the cross-sectional area of the thickest region in the BLM-treated lung had decreased to approximately 64.2 %. Thus, BLM administration had a remarkable impact on both the internal structure and the overall size of the lungs.

4. Discussion

This study introduces a novel method for administering aerosol to *Xenopus* through inhalation. Furthermore, the effects of administering BLM, a drug known to artificially induce pulmonary fibrosis in mammals, were observed and evaluated. The results, based on observations of the lungs' external appearance, internal observations using tissue sections and simple sections, and HE staining, confirmed that symptoms similar to pulmonary fibrosis were indeed induced by BLM administration. Future applications, such as administering other drugs, are anticipated.

Since BLM administration was first implemented in dogs (Fleischman et al., 1971), it has been used in mammals (mice, rats, dogs, sheep, monkeys, pigs, etc.) and fish (zebrafish). This study shows that it can now also be applied to amphibians (*Xenopus*). About half a century ago, inflammation could only be confirmed through histological methods such as HE staining (Fleischman et al., 1971). HE stains the cytoplasm and nuclei, allowing for direct observation of how the cells of the specimen have changed. However, it is a staining method that requires maintaining consistent quality through many processes and demands a certain level of skill (Wick, 2019). Additionally, tissue distortion or uneven staining can occur due to stretching or reagent degradation, making it qualitative in nature.

In recent years, with advances in analysis techniques in the BLM administration model, RNA sequencing has made great progress as a complementary method to qualitative analysis (Bian et al., 2023; Liu et al., 2021). RNA sequencing reads mRNA sequences comprehensively and converts them into data, allowing for the identification of genes that are differentially expressed when compared to the Control group. In mouse models, the release and identification of inflammatory cytokines (particularly IL-6, IL-1ß, and Tgf-ß1), chemokines, and the activation of inflammatory cells following BLM administration have been reported using single-cell RNA sequencing (Bian et al., 2023; Moore and Hogaboam, 2008). In these studies, both human and mouse lungs exhibited a reduction in FOXF1-

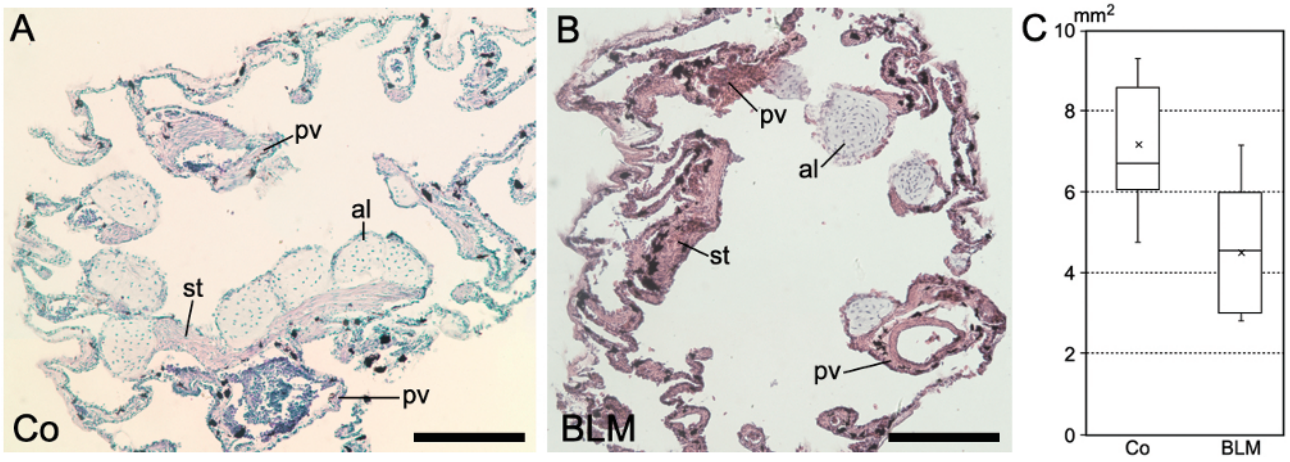

Fig. 4 BLM administration affects alveolar formation and reduces lung thickness
(A) Tissue section of the Control lung. Section cut at the site indicated by the dotted line in Fig. 3A. (B) Tissue section of the BLM-treated lung. Section cut at the site indicated by the dotted line in Fig. 3B. Both A and B are shown at 40x magnification, and the scale bar represents 20 µm. al, alveoli; pv, pulmonary vessels; st, stroma. (C) Comparison of the cross-sectional area of the thickest part of the lung in tissue sections. The average cross-sectional area of the thickest part of the Control lung was approximately 7.21 mm^2, while that of the BLM-treated lung was approximately 4.63 mm^2 (both n=15, $p < 0.00005$).

expressing endothelial cells following bleomycin exposure, indicating a similarity in gene expression across species regarding fibrotic processes. This suggests that the molecular mechanisms driving pulmonary fibrosis, including the downregulation of FOXF1, are conserved between mice and humans. Similar results may also be observed in experimental systems using *Xenopus*. In the future, the effects of BLM administration on the lungs of *Xenopus* will also be quantified through molecular biological methods.

Acknowledgments

This study was made possible with the support of Human Life CORD JAPAN Inc. I would also like to express my heartfelt gratitude to Honori Ishikawa and Teruyuki Saita, graduates of our laboratory, who conducted many of the foundational experiments.

References

Alves-Pimenta, S., Colaço, B., Oliveira, P. A., Venâncio, C. (2024) “Development Features on the Selection of Animal Models for Teratogenic Testing”, *Methods Mol. Biol.*, 2753, p.67-104.

Bian, F., Lan, Y., Zhao, S., Deng, Z., Shukla, S., et al. (2023) “Lung endothelial cells regulate pulmonary fibrosis through FOXF1/R-Ras signaling”, *Nat. Commun*., 14, 2560.

Dietert, K., Gutbier, B., Wienhold, S. M., Reppe, K., Jiang, X., et al. (2017) “Spectrum of pathogen- and model-specific histopathologies in mouse models of acute pneumonia”, *PLoS One*, 12, e0188251.

Fleischman, R. W., Baker, J. R., Thompson, G. R., Schaeppi, U. H., Illievski, V. R., et al. (1971) “Bleomycin-induced interstitial pneumonia in dogs”, *Thorax*, 26, p.675-82.

Li, Y., Chen, J., Chen, X., Wang, L., Gautam, S., et al. (2002) “Human marrow stromal cell therapy for stroke in rat: neurotrophins and functional recovery”, *Neurology*, 59, p.514-23.

Liu, X., Qin, X., Qin, H., Jia, C., Yuan, Y., et al. (2021) “Characterization of the heterogeneity of endothelial cells in bleomycin-induced lung fibrosis using single-cell RNA sequencing”, *Angiogenesis*, 24, p.809-21.

Moeller, A., Ask, K., Warburton, D., Gauldie, J., Kolb, M. (2007) “The bleomycin animal model: a useful tool to investigate treatment options for idiopathic pulmonary fibrosis?”, *Int. J. Biochem. Cell Biol*., 40, p.362-82.

Moore, B. B. and Hogaboam, C. M. (2008) “Murine models of pulmonary fibrosis”, *Am. J. Physiol. Lung Cell Mol. Physiol.*, 294, p.152-60.

Nenni, M. J., Fisher, M. E., James-Zorn, C., Pells, T. J., Ponferrada, V., et al. (2019) “Xenbase: Facilitating the Use of Xenopus to Model Human Disease”, *Front Physiol.*, 10, 154. [PMID: 30863320]

Odelberg, S. J. (2005) “Cellular plasticity in vertebrate regeneration”, *Anat. Rec B New Anat*. 287, p.25-35.

Rankin, S. A., Thi Tran, H., Wlizla, M., Mancini, P., Shifley, E. T., et al. (2015) “A Molecular atlas of *Xenopus* respiratory system development”, *Dev. Dyn*., 244, p.69-85.

Sanjeewa, K., Jayawardena, T. U., Lee, H. G., Herath, K., Jee, Y., et al. (2019) “The protective effect of Sargassum horneri against particulate matter- induced inflammation in lung tissues of an in vivo mouse asthma model”, *Food Funct.*, 10, p.7995-8004.

Shen, Z., Su, T., Chen, J., Xie, Z., Li, J. (2021) “Collagen triple helix repeat containing-1 exerts antifibrotic effects on human skin fibroblast and bleomycin-induced dermal fibrosis models”, *Ann. Transl. Med*., 9, p.801.

Stubbe, J. and Kozarich, J. W. (1987) “Mechanisms of bleomycin-induced DNA degradation”, *Chem. Rev*., 87, p.1107-36.

Umezawa, H. (1974) “Chemistry and mechanism of action of bleomycin” , Fed. Proc., 33, p.2296-302.

Warburton, D., El-Hashash, A., Carraro, G., Tiozzo, C., Sala, F., et al. (2010) “Lung organogenesis”, *Curr. Top. Dev. Biol*., 90, p.73-158.

Wick, M. R. (2019) “The hematoxylin and eosin stain in anatomic pathology-An often-neglected focus of quality assurance in the laboratory”, *Semin. Diagn. Pathol*., 36, p.303-11.

Wolters, P. J., Collard, H. R., Jones, K. D. (2014) “Pathogenesis of idiopathic pulmonary fibrosis”, *Annu. Rev. Pathol*., 9, p.157-79.

〔受付日　2024. 9. 30〕
〔採録日　2024. 10. 25〕